International Journal of Heat and Mass Transfer 140 (2019) 129–138

Contents lists available at ScienceDirect

International Journal of Heat and Mass Transfer

journal homepage: www.elsevier.com/locate/ijhmt

Experimental investigation on the Reynolds dependence of the performance of branched heat exchangers working with organic fluids

R. Capata *, L. Gagliardi

University of Roma "Sapienza", Department of Mechanical and Aerospace Engineering, Italy

ARTICLE INFO

Article history:
Received 8 August 2018
Received in revised form 30 May 2019
Accepted 30 May 2019

Keywords:
Experimental test
Branched heat exchanger
Constructal theory
Exchanger efficiency
Load losses
Exchangers comparison
Organic fluid

ABSTRACT

The aim of this work is to continue the experimental evaluation of three different compact branched heat exchangers. To complete the previous study, additional experimental tests were carried out, using a commercial automotive refrigerant (Glycol) at different concentrations (50%, 100%). Finally, in order to have a deeper knowledge of this phenomenon and to identify the parameters regulating the heat transfer, an organic fluid has also been used and tested. The use of such a fluid has required a re-elaboration and design of the test bench. In fact, a vacuum circuit has been realized to properly use the organic fluid. As a result, the equipment used has been changed and inserting more sophisticated sensors. Finally, once all the tests have been completed, the various dimensionless parameters, characterizing the heat exchange, have been calculated and a comparative evaluation has been carried out, to determine and propose the optimal configuration of the branched heat exchanger.

1. Introduction

The aim of this work is to continue and improve the identification of the optimal configuration for a branched heat exchanger, using different refrigerant fluids. In a previous work, three different configurations have been investigated [1–5]. The three configurations are similar, but differ in the internal channels geometry. Referring to Fig. 1, the heat exchangers are composed of two facing disks; on each disk, semi-circular channels are obtained, to realize a circular-shaped one, when the two disks are assembled. The fluid enters through a hole on the upper disc and crosses the heat exchanger inner channels. Two branching levels are considered, for a total of six channels after the first bifurcation and twelve channels after the second one. The twelve output channels are equally distributed along the exchanger circumference, with a 30° overlapping. The comparison of three configurations was performed for three different flow rates: 2 l/min, 4 l/min and 10 l/min. To achieve a more reliable comparison, several tests were carried out for each heat exchanger and for each mass flow rate so that the validity of the final results could be evaluated statistically [6–8].

2. Geometry description

A very brief description of the devices, considered in the tests, is presented. Each exchanger configuration is characterized by the following common dimensions:

- Disk diameter D = 150 mm
- Thickness disk s = 15 mm
- Initial channel diameter D_0 = 12.96 mm
- Initial length L_0 = 11.20 mm (obtained by scaling the model proposed in [2])

While for the branches inner diameters (D_1 and D_2) and lengths (L_1 and L_2) three different configurations are so defined:

2.1. Constant mean velocity configuration (A)

- D_1 = 9.16 mm
- D_2 = 6.48 mm
- L_1 = 41.3 mm
- L_2 = 29.2 mm

2.2. Constant Reynolds configuration (B)

- D_1 = 6.48 mm
- D_2 = 3.24 mm

* Corresponding author.
E-mail address: roberto.capata@uniroma1.it (R. Capata).

https://doi.org/10.1016/j.ijheatmasstransfer.2019.05.114
0017-9310/

Nomenclature

Al	aluminum
c	water specific heat [J/kg K]
C	constant
D	diameter [m]
L	channel length [m]
m	mass flow rate [l/min]
Mn	manganese
N	measures number
Nu	Nusselt number
p	pressure [bar]
P	power [W]
Pr	Prandtl number
Re	Reynolds number
s	thickness [m]
T	temperature [°C]
U	fluid velocity within the exchanger [m/s]
x	generic measurement value

Greek symbols

Δ	difference
μ	dynamic viscosity [kg/m s]
η	efficiency
ρ	density [kg/m^3]
σ_x	standard deviation

Subscripts

0	initial diameter, initial channel length
1	diameter or length before bifurcations
2	diameter or length after bifurcations
1,. . .,12	measure points
amb	ambient
in	inlet
i	ith value
j	jth = ith + 1 value
m	average, medium
out	outlet

- L_1 = 48.52 mm
- L_2 = 24.26 mm

2.3. Constructal configuration (C)

- D_1 = 10.28 mm
- D_2 = 8.16 mm
- L_1 = 38.46 mm
- L_2 = 31.41 mm

All three exchangers are aluminum made. The alloy properties have already been described in a previous work and have been compared with those presented in [9]. The value of length L_0 is obtained by scaling the model proposed in [2,10,11] (see Figs. 2–4).

3. Test bench assembling and new experimental campaign

In the previous work [5], the entire test bench had been described. Fig. 5 show the layout of the test bench. The test campaign was focused on the measurement of thermal exchange efficiency, the calculation of load losses and the determination of pre-stabilization time.

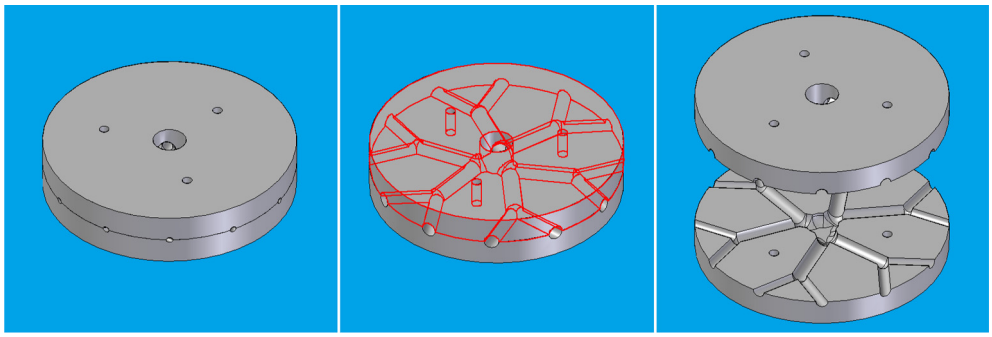

Fig. 1. Compact branched heat exchanger.

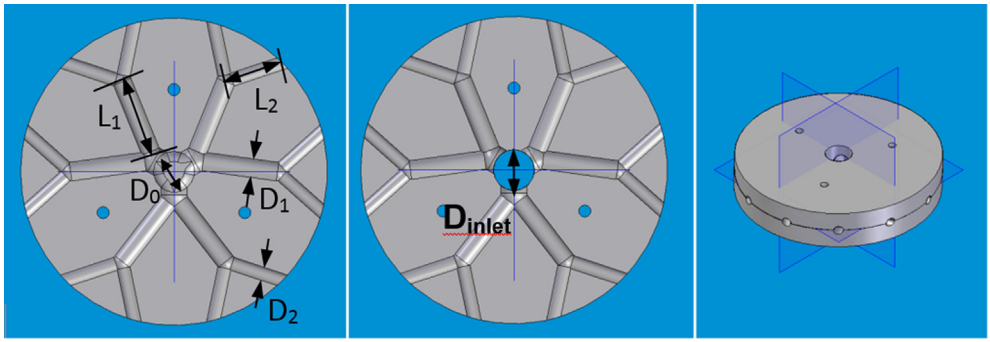

Fig. 2. Heat exchanger configuration A.

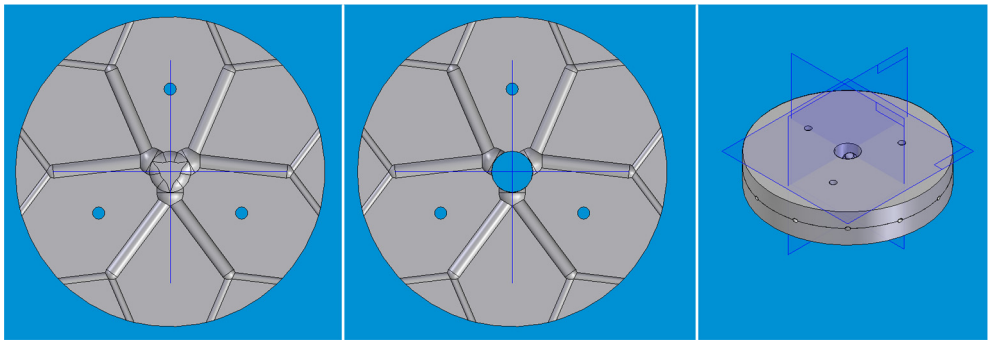

Fig. 3. Configuration B heat exchanger.

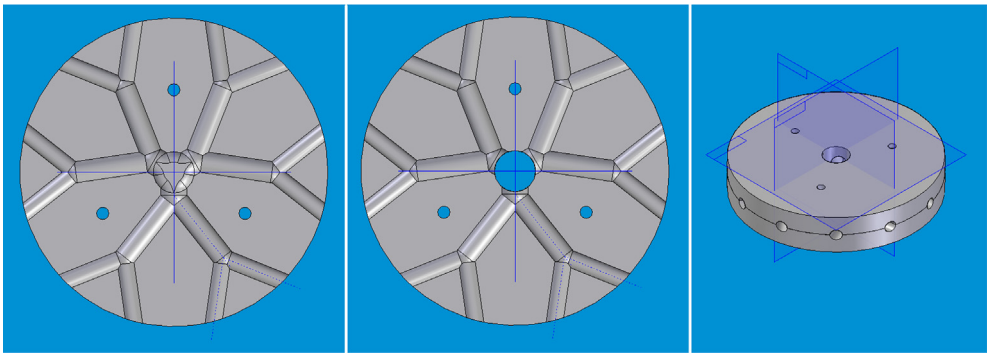

Fig. 4. Configuration C heat exchanger.

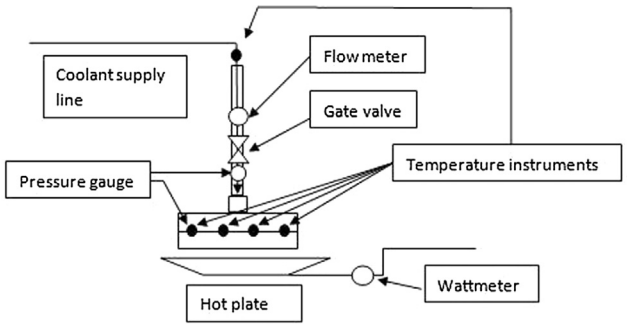

Fig. 5. Concept layout of the test bench.

The main parts are:

- Refrigerant fluid tank.
- Hot plate with a power of 500 W.
- Submersible pump.
- Flowmeter.

The instrumentations used are:

- Thermocouple SE011 PT100, Class A.
- Bourdon EN 837-1 pressure gauge.
- Wattmeter.

3.1. Common refrigerant fluids

The tests have been carried out with the three different heat exchangers, using different refrigerants. Compared to previous work [5], 100% ethylene glycol fluid was added. The considered refrigerants are:

(1) Water;
(2) Low Density Oil;
(3) Bio 46 ES Fluid (High Density Oil);
(4) Water mixed with Ethylene Glycol (Mixed at 50%);
(5) 100% Ethylene Glycol.

Table 1 summarizes all operating fluid properties.

Table 1
Fluids specifications.

Water			
Density $\left[\frac{kg}{m^3}\right]$	Viscosity [cP]	Boiling point [°C]	Melting point [°C]
997 at 20 °C	1.1 at 20 °C	100	0
Low Density Oil			
Density $\left[\frac{kg}{m^3}\right]$		Viscosity [cP]	
920 at 20 °C		37.1 at 25 °C	
Bio 46 ES fluid (High Density Oil)			
Density $\left[\frac{kg}{m^3}\right]$		Viscosity [cP]	
962 at 20 °C		46 at 25 °C	
Ethylene Glycol			
Density $\left[\frac{kg}{m^3}\right]$		Viscosity [cP]	
1100 at 20 °C		21 at 25 °C	

3.2. Thermal field

The first result was the congruency with the previous experiments results. Consequently, the procedure proposed for tests can be considered satisfactory. Moreover, in Table 2 (where T_{in} indicates the inlet fluid temperature into the exchanger; $T_1, \ldots, T_{12}$ indicate the outlet fluid temperature from channels; T_{ex} indicates the exchanger temperature at steady state conditions) the values of a random test are reported (#7 of a 15 series test, for each exchanger).

3.3. Viscous losses and elapsed time

Proceeding as described in [5], the values of the pressure drop and the experiment elapsed time are reported in Table 3. In the table, p_{in} indicates the upstream pressure of the heat exchanger and p_{out} the exchanger outlet pressure, expressed in bars. In the last column reports the elapsed time.

3.4. Data treatment and normalization

A 15 tests series for each value of mass flowrate and for each heat exchanger have been carried out. All data has been collected via PC and processed [7–9]:

(a) Gauss Analysis of the deviations: mean values, mode, median and standard deviation have been automatically calculated by the acquisition card software;
(b) Filtering: each data that exceeded 3σ has been individually controlled by software, and neglected like spur if possible acquisition errors were not found;
(c) Normalization: the values are standardized in order to control that their distribution followed a Gaussian- type;
(d) Presentation**:** for each measure, the relative standard deviation and the medium value has been calculated (“rms”).

All these phase have been carried out by the software.

4. Assembling of a new TEST BENCH for testing an organic fluid (R134a)

For the new refrigerant, a study of its thermo-fluid dynamics properties is mandatory. The main problem concerns the initial conditions: in fact, to perform a comparison between this test and the previous ones (with operating fluids) it is necessary that, at exchanger inlet, the fluid temperature and the condition are the same or very close. Anyway, in these series of tests, it is not possible to set the flow-rate by means of a flow-meter, due to

Table 2
Thermal field results.

Fluid	Type	Q [l/min]	T_{in} [°C]	T_{ex} [°C]	T_1 [°C]	T_2 [°C]	T_3 [°C]	T_4 [°C]	T_5 [°C]	T_6 [°C]	T_7 [°C]	T_8 [°C]	T_9 [°C]	T_{10} [°C]	T_{11} [°C]	T_{12} [°C]
Water	A	2	31	47	36.5	36.8	36.6	36.7	36.6	36.5	36.7	36.6	36.7	36.6	36.5	36.7
	B	2	31.	47	33.1	33.1	33.2	33.1	33.3	33.1	33.1	33.2	33.2	33.2	33.2	33.2
	C	2	35.9	53.3	40.4	40.3	40.3	40.4	40.2	40.4	40.2	40.3	40.3	40.2	40.2	40.3
	A	4	36	45.8	38.3	38.4	38.4	38.3	38.5	38.4	38.5	38.6	38.4	38.5	38.4	38.5
	B	4	36	46.4	36.6	36.6	36.6	36.6	36.6	36.6	36.6	36.6	36.6	36.6	36.6	36.6
	C	4	38.8	49.8	42.6	42.7	42.6	42.7	42.6	42.7	42.6	42.7	42.6	42.7	42.6	42.7
	A	10	39	42	39.8	39.8	39.9	39.8	39.8	39.7	39.8	39.8	39.7	39.7	39.8	39.8
	B	10	39.2	45.7	39.6	39.6	39.7	39.6	39.7	39.6	39.8	39.5	39.5	39.6	39.5	39.8
	C	10	39.7	46.7	43.3	43.2	43.3	43.4	43.2	43.3	43.4	43.3	43.2	43.2	43.4	43.3
Low Density Oil	A	2	28.1	83.8	31.2	31.2	31.3	31.2	31.2	31.1	31.2	31.2	31.3	31.3	31.2	31.2
	B	2	29.2	91.6	32.2	32.2	32.3	32.3	32.3	32.3	32.1	32.2	32.2	32.2	32.2	32.2
	C	2	29.8	91.6	35.5	35.5	35.3	35.3	35.3	35.3	35.6	35.3	35.3	35.3	35.6	35.3
	A	4	31	79.2	33.6	33.6	33.6	33.5	33.6	33.5	33.7	33.6	33.7	33.6	33.6	33.6
	B	4	32.4	85.9	34.8	34.8	34.8	34.9	34.9	34.7	34.7	34.7	34.7	34.8	34.8	34.8
	C	4	36.7	85.8	38.8	38.8	38.9	38.3	38.8	38.8	38.9	38.9	38.8	38.8	38.8	38.9
	A	10	34.8	67.4	36.1	36	36	36	36.1	36.1	36	36	36	36	36	36
	B	10	36.9	78.5	38.1	38.1	38.2	38.2	38.1	38.2	38.2	38.1	38.1	38.1	38.1	38.2
	C	10	40.1	79.5	40.3	40.3	40.3	40.2	40.3	40.3	40.3	40.3	40.2	40.2	40.3	40.3
Bio 46 ES Fluid	A	2	27.6	76.3	30.3	30.3	30.3	30.2	30.2	30.3	30.3	30.2	30.2	30.3	30.2	30.3
	B	2	29.7	76.7	31.2	31.2	31.3	31.2	31.2	31.3	31.3	31.3	31.2	31.2	31.2	31.3
	C	2	27.2	75.1	33.5	33.5	33.5	33.6	33.5	33.5	33.5	33.5	33.5	33.6	33.5	33.63
	A	4	33.3	75.9	34.2	34.2	34.2	34.2	34.3	34.3	34.2	34.2	34.3	34.3	34.3	34.2
	B	4	35	73.7	35.8	35.8	35.8	35.8	35.7	35.7	35.8	35.7	35.8	35.8	35.8	35.7
	C	4	33.1	67.6	35.3	35.3	35.3	35.4	35.4	35.3	35.3	35.3	35.3	35.3	35.4	35.4
	A	10	37.7	71.2	38.3	38.3	38.3	38.2	38.2	38.2	38.3	38.3	38.3	38.3	38.3	38.3
	B	10	37.6	71.3	38.2	38.3	38.2	38.2	38.3	38.2	38.3	38.2	38.2	38.3	38.2	38.2
	C	10	36.2	60.7	36.9	36.9	36.9	36.8	36.9	36.8	36.8	36.8	36.9	36.9	36.8	36.8
Ethylene Glycol + Water	A	2	22.4	33.7	23	23	23	23.1	23	23	23.1	23	23.1	23	23.1	23
	B	2	22.4	37.3	24	24	24	24	24.1	23.9	24	24.1	23.9	24	24	24
	C	2	24.1	36.4	25.6	25.6	25.6	25.6	25.5	25.5	25.5	25.6	25.5	25.6	25.6	25.6
	A	4	24	31.2	24.3	24.3	24.2	24.3	24.3	24.2	24.2	24.2	24.3	24.3	24.2	24.2
	B	4	23.9	35.6	25.3	25.3	25.4	25.3	25.3	25.3	25.3	25.3	25.4	25.4	25.3	25.3
	C	4	26.3	35.2	27.7	27.7	27.7	27.6	27.6	27.6	27.6	27.7	27.7	27.7	27.6	27.6
	A	10	25.9	29.9	26	26	26	26.1	26.1	26	26.1	26	26	26	26	26
	B	10	25.2	34.6	26	26	26	26	26.1	26.1	26.1	26.1	26	26	26.1	26
	C	10	28.2	34.9	28.4	28.4	28.3	28.3	28.4	28.4	28.4	28.4	28.3	28.3	28.4	28.4
100% Ethylene Glycol	A	2	21.2	29.7	21.6	21.7	21.6	21.6	21.7	21.6	21.7	21.7	21.6	21.6	21.7	21.6
	B	2	22.4	37.3	24	24	24	24	24.1	23.9	24	24.1	23.9	24	24	24
	C	2	24.1	36.4	25.6	25.6	25.6	25.6	25.5	25.5	25.5	25.6	25.5	25.6	25.6	25.6
	A	4	24	31.2	24.3	24.3	24.2	24.3	24.3	24.2	24.2	24.2	24.3	24.3	24.2	24.2
	B	4	23.9	35.6	25.3	25.3	25.4	25.3	25.3	25.3	25.3	25.3	25.4	25.4	25.3	25.3
	C	4	26.3	35.2	27.7	27.7	27.7	27.6	27.6	27.6	27.6	27.7	27.7	27.7	27.6	27.6
	A	10	25.99	29.9	26	26	26	26.1	26.1	26	26.1	26	26	26	26	26
	B	10	25.2	34.6	26	26	26	26	26.1	26.1	26.1	26.1	26	26	26.1	26
	C	10	28.2	34.9	28.4	28.4	28.3	28.4	28.4	28.4	28.4	28.4	28.3	28.3	28.4	28.4

Table 3
Load losses and experiment time for the different operating fluids.

Fluid	Type	Q [l/min]	p_{in} [bar]	p_{out} [bar]	Time [s]
Water	A	2	<0.002	<0.002	252
	B	2	<0.002	<0.002	325
	C	2	<0.002	<0.002	263
	A	4	<0.002	<0.002	215
	B	4	<0.002	<0.002	300
	C	4	<0.002	<0.002	233
	A	10	<0.002	<0.002	203
	B	10	<0.002	<0.002	273
	C	10	<0.002	<0.002	197
Low density oil	A	2	<0.002	<0.002	357
	B	2	<0.002	<0.002	430
	C	2	<0.002	<0.002	368
	A	4	<0.002	<0.002	320
	B	4	<0.002	<0.002	405
	C	4	<0.002	<0.002	338
	A	10	<0.002	<0.002	320
	B	10	<0.002	<0.002	405
	C	10	<0.002	<0.002	338
Bio 46 ES Fluid	A	2	<0.002	<0.002	320
	B	2	<0.002	<0.002	405
	C	2	<0.002	<0.002	338
	A	4	<0.002	<0.002	265
	B	4	<0.002	<0.002	350
	C	4	<0.002	<0.002	283
	A	10	<0.002	<0.002	265
	B	10	<0.002	<0.002	350
	C	10	<0.002	<0.002	283
Ethylene glycol + water	A	2	<0.002	<0.002	177
	B	2	<0.002	<0.002	250
	C	2	<0.002	<0.002	188
	A	4	<0.002	<0.002	140
	B	4	<0.002	<0.002	225
	C	4	<0.002	<0.002	158
	A	10	<0.002	<0.002	128
	B	10	<0.002	<0.002	198
	C	10	<0.002	<0.002	122
100% Ehtylene glycol	A	2	<0.002	<0.002	141
	B	2	<0.002	<0.002	224
	C	2	<0.002	<0.002	157
	A	4	<0.002	<0.002	103
	B	4	<0.002	<0.002	201
	C	4	<0.002	<0.002	122
	A	10	<0.002	<0.002	97
	B	10	<0.002	<0.002	178
	C	10	<0.002	<0.002	110

constructive problems. The mass flow rate is set by a compressor, connected to an inverter. The selected values are 0.22, 0.27 and 0.33 l/min. Moreover, this fluid results non-flammable and non-explosive, so it can be used in total safety conditions.

4.1. R134a properties

The following Pressure-Enthalpy diagram (Fig. 6) reports the thermodynamic characteristics of the refrigerant fluid. Red lines fluid temperature [°C], green lines to specific volume [m^3/kg] and blue lines to specific entropy [kJ/kg K]. Table 4 lists the numerical values of the thermodynamic properties of the saturated fluid. Where "v_f" is the specific volume of liquid, "v_g" is the specific volume of gas, "h_f" is the liquid enthalpy, "h_{fg}" is the liquid-gas enthalpy and "hg" is the gas enthalpy.

4.2. Initial conditions

Considering the initial conditions of 20 °C, the following table shows the liquid state of aggregation and the fluid operating values. It has been necessary to compress the fluid, to reach the correct initial conditions at the exchanger inlet. Then, to ensure that the incoming fluid continuously complies with the initial conditions, a refrigeration cycle has been realized [12–14].

4.3. Refrigeration cycle

The cycle consists in 4 phases: Compression, Condensation, Expansion and Evaporation. Each of these phases has been designed, to allow correct operation of the heat exchanger, in full compliance with safety. These phases are described below:

1. Compression: in this phase the transformation is assumed as an isentropic compression from 5.7171 bar (at 30 °C) to 19.8 bar (at 80 °C). The fluid is gaseous;
2. Condensation: this transformation allows the fluid to pass from a gaseous to a liquid state. Condensation starts at 80 °C (at 19.8 bar) and finishes at 57 °C (19.8 bar);
3. Expansion: the fluid has a pressure and temperature drop, remaining in the liquid state. This transformation is assumed as an isenthalpic expansion and starts at 19.8 bar (at 57 °C) and finishes at 5.7171 bar (at 20 °C). The fluid is a mix of liquid and gas, with a high liquid concentration;

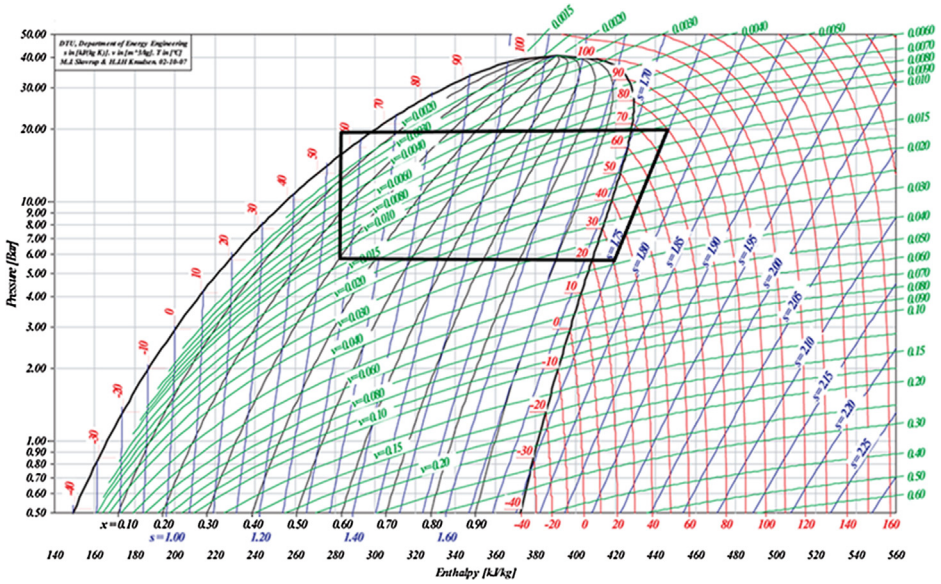

Fig. 6. Refrigerant cycle on p_h diagram.

Table 4
Refrigeration cycle initial conditions.

Temperature [°C]	Pressure [bar]	State of aggregation	Initial conditions
20	1.01325	Gas	Verified
20	6	Liquid	Verified

4. Evaporation: this phase is closely related to this work. In fact, the fluid enters the branched heat exchanger at 20 °C (at 5.7171 bar), as liquid. Here the cooling of the heat source takes place. The refrigerant leaves the exchanger at a temperature of 30 °C (5.7171 bar) as a gas.

All these phases are represented in the refrigeration cycle (Fig. 6). In the cycle properties calculation, the following parameters have been considered:

- Thermal power = 500 W
- Specific isobar heat capacity at 20 °C = 1.44 kJ/kg K

4.4. Real refrigeration cycles

For safety reasons it was not possible to realize the previously described cycle. In fact, if an elevated operating pressure is reached at the inlet section, there is a risk of cooling system and measuring instruments damage. Therefore, a lower inlet pressure was selected, which led to a consequent fluid temperature decrease. The "new" refrigeration cycles, listed for each different flow-rate are reported in Tables 5–7.

4.5. The test bench

The new test bench reproduces, as possible, the previous one (Fig. 7).

The main differences are:

- Pressurized refrigerant supply circuit
- Improved Measurement system
- Electrical circuit for the compressor regulation and control

The test bench has been assembled at University Laboratory. The components are:

- Hot plate with a power of 500 W (already used in the previous tests);
- Hermetic reciprocating compressor;
- Frequency inverter;
- Capillary pipe and dehydrator filter;

Table 5
Cycle (A): 0.33 l/min.

Phase	Initial aggregation status	Final aggregation status	Initial temp. [°C]	Final temp. [°C]	Initial pressure [bar]	Final pressure [bar]
Compression	Gas	Gas	34	91	2	10.2
Condensation	Gas	Liquid	91	30	10.2	10.2
Expansion	Liquid	Liquid & Gas	30	−10	10.2	2
Evaporation	Liquid & Gas	Gas	−10	34	2	2

Table 6
Cycle (B): 0.27 l/min.

Phase	Initial aggregation status	Final aggregation status	Initial temp. [°C]	Final temp. [°C]	Initial pressure [bar]	Final pressure [bar]
Compression	Gas	Gas	44	96	2.2	10.2
Condensation	Gas	Liquid	96	35	10.2	10.2
Expansion	Liquid	Liquid & Gas	35	−8	10.2	2.2
Evaporation	Liquid & Gas	Gas	−8	44	2.2	2.2

Table 7
Cycle (C): 0.22 l/min.

Phase	Initial aggregation status	Final aggregation status	Initial temp. [°C]	Final temp. [°C]	Initial pressure [bar]	Final pressure [bar]
Compression	Gas	Gas	57	101	2.35	10.2
Condensation	Gas	Liquid	101	41	10.2	10.2
Expansion	Liquid	Liquid & Gas	41	−6	10.2	2.35
Evaporation	Liquid & Gas	Gas	−6	57	2.35	2.35

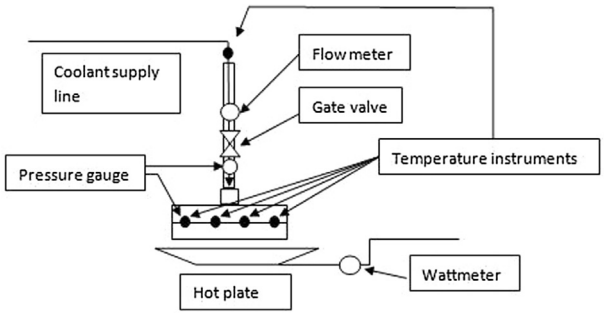

Fig. 7. Test bench conceptual sketch and refrigerant circuit.

- Condenser;
- Inlet/Outlet valve

The detailed description of each single component is listed in the following Tables 8–10.

The presence of capillary tube is necessary during the expansion phase. In addition, it is necessary a dehydrator filter to remove the moisture present in the circuit. The condenser is composed of a series of tubes arranged in serpentine. Table 10 reports the various technical components features.

Table 8
Compressor nameplate.

Power range	0.1–0.2 kW
Displacement	6.6 cm^3
Nominal voltage and frequency	220–240 V 50–60 Hz
Gas flow rate	6.27–19.21 kg/h
Cooling capacity	261–938 W
Operating pressure (gauge)	15.85 bar
Peak pressure (gauge)	20.2 bar
Rpm range	2300–3600 rpm

Table 9
Inverter nominal data.

Input offset voltage [V]	230
Output rating (max) [kW]	0.75
Frequency range [Hz]	0–650

Table 10
Component technical data.

Capillary pipe & Dehydrator		Condenser	
Material	Alloy	Material	Alloy
Length [m]	1.6	Dimensions [m]	0.7 × 0.306 × 0.026
Inner diameter [m]	0.9	Max. operating pressure [bar]	40
Pressure drop range [bar]	5–8		

5. Organic fluid experimental campaign

In this experimental campaign, tests were carried out using organic fluid. Because of the different operating conditions and the different instruments used, the test procedures are different.

5.1. Organic fluid measurement instruments

The instruments used to measure the thermal efficiency and the pressure drop are:

- Thermocouples SE011 PT100, Class A.
- Thermocouple RS-PRO
- Pressure gauges.

5.2. Thermal heat exchangers efficiency experimental campaign procedure

A hot plate with a 500 W nominal output power was used (as in the previous tests). The coolant fluid is an organic refrigerant fluid. The experiment procedure is:

(1) Connect the refrigerant supply system to the chosen heat exchanger;
(2) Connect the refrigerant vacuum/input device through the inlet/outlet valve;
(3) Vacuum the refrigeration circuit;
(4) Insert the organic fluid inside the circuit;
(5) Disconnect the refrigerant vacuum/input device from the valve;
(6) Turn on the hot plate to heat the exchanger for 5 min until to reach 100 °C of disk temperature (measured value);
(7) Connect the compressor to the power supply;
(8) Set the frequency on the inverter;
(9) Wait for the new steady conditions achievement;
(10) Outlet fluid temperature measurements (for each output channel.); Table 11
(11) Inlet fluid and ambient temperature measurements;
(12) Disassemble the heat exchanger from the compressor's input and output;

5.3. Campaign elapsed time

These tests have been carried out simultaneously with the other tests. The time that the system needs to reach the stationary working condition has been measured following these steps:

(1) Wait until the system reaches the temperature of 100° C;
(2) Connect the compressor to the power supply;
(3) Set the frequency on the inverter;
(4) Start the chronometer;
(5) Wait for stationary working condition of the system;
(6) Stop the chronometer;
(7) Read and Write the time vested by the chronometer;

Table 11
Temperature fields.

Fluid	Type	Q [l/min]	T_{in} [°C]	T_{ex} [°C]	T_1 [°C]	T_2 [°C]	T_3 [°C]	T_4 [°C]	T_5 [°C]	T_6 [°C]	T_7 [°C]	T_8 [°C]	T_9 [°C]	T_{10} [°C]	T_{11} [°C]	T_{12} [°C]
R134a	A	0.22	−6	27.8	57.1	57.2	57.1	57.2	57.1	57.2	57.1	57.2	57.1	57.2	57.1	57.1
	B	0.22	−6	29.9	58.6	58.7	58.6	58.7	58.7	58.6	58.7	58.6	58.7	58.6	58.6	58.7
	C	0.22	−6	53.4	99.2	99.3	99.2	99.3	99.2	99.3	99.3	99.2	99.3	99.2	99.3	99.2
	A	0.27	−8	20.3	44.1	44.2	44.2	44.2	44.1	44.1	44.2	44.1	44.1	44.2	44.1	44.2
	B	0.27	−8	22.3	45.3	45.2	45.2	45.3	45.2	45.3	45.2	45.3	45.3	45.3	45.2	45.3
	C	0.27	−8	40.7	85.7	85.6	85.7	85.6	85.7	85.7	85.7	85.7	85.6	85.6	85.6	85.7
	A	0.33	−10	13.9	33.3	33.4	33.4	33.3	33.2	33.5	33.3	33.2	33.4	33.3	33.4	33.4
	B	0.33	−10	15.2	33.2	33.2	33.4	33.3	33.3	33.4	33.2	33.2	33.2	33.2	33.2	33.3
	C	0.33	−10	30.8	67.9	68	68.1	68	67.9	68.1	68	68	67.9	62.1	68	68.1

Table 12
Pressure loss and test time.

Fluid	Type	Q [l/min]	p_{in} [bar]	p_{out} [bar]	Time [s]
R134A – Tetrafluoroethane	A	0.22	2.34	2.34	130
	B	0.22	2.34	2.34	160
	C	0.22	2.34	2.34	152
	A	0.27	2.17	2.17	101
	B	0.27	2.17	2.17	132
	C	0.27	2.17	2.17	130
	A	0.33	2	2	92
	B	0.33	2	2	110
	C	0.33	2	2	106

Table 13
Fluid proprieties.

Fluid/Proprieties	Water	Low density oil	Bio 46 ES	Ethylene glycol	Organic fluid
Density [kg/m^3]	994	920	962	1110	971.5
Dynamic viscosity [cP]	1.1	37.1	46	21	0.22

Table 14
Configuration comparison.

	U = Cost.	Re = Cost.	Constructal
Water	X		
Low density Oil	X+		X
Bio 46 ES fluid	X		X+
50% Glycol + 50% Water	X		
100%Ethylene Glycol	X		

5.4. Head losses experimental campaign

For the pressure drop, two pressure gauges were used. The first one is located near the exchanger input, to measure the inlet pressure. The second one is positioned on the heat exchanger, in an appropriate hole. The procedure is:

(a) Connect the compressor to the power supply;
(b) Set the frequency on the inverter;

Table 15
Calculated Reynolds/Prandtl numbers.

Fluid	Reynolds			Prandtl		
	U = Cost.	Re = Cost.	Constructal	U = Cost.	Re = Cost.	Constructal
Water	2353	2936	1863	7.6	7.6	7.6
Low density oil	654.4	803.5	509.8	516.3	516.3	516.3
Bio 46 ES fluid	536.7	677.4	481.2	552	552	552
Water-glycol	1553	1712.3	1086	29.7	29.7	29.7
100% Ethylene glycol	1352.5	1707	1212.6	198.2	198.2	198.2

Table 16
Calculated Reynolds/Prandtl numbers for R134 fluid.

R134 flow rate [l/min]	Reynolds			Prandtl		
	U = Cost.	Re = Cost.	Constructal	U = Cost.	Re = Cost.	Constructal
First branch						
0.22	2235	3162	1993	3.53	3.53	3.53
0.27	2794	3953	2492	3.53	3.53	3.53
0.33	3355	1569	2992	3.53	3.53	3.53
Second branch						
0.23	1581	3162	1255	3.53	3.53	3.53
0.27	3148	3953	1569	3.53	3.53	3.53
0.33	2373	4764	1884	3.53	3.53	3.53

Table 17
Nusselt number.

Fluid	Nusselt		
	U = Cost.	Re = Cost.	Constructal
Water	157.21	146.48	138.47
Low density oil	78.40	70.89	76.77
Bio 46 ES fluid	75.04	68.47	77,01
Water-glycol	218.20	208.83	184.29
100% Ethylene glycol	391.74	376.33	362.39

Table 18
Nusselt number.

R134 flow rate [l/min]	Nusselt		
	U = Cost.	Re = Cost.	Constructal
First branch			
0.22	146.4509	117.2137	100.6491
0.27	158.6296	127.1391	109.2342
0.33	135.8042	113.2882	116.7189
Second branch			
0.23	146.4509	103.133	84.69697
0.27	158.6296	132.7324	92.10422
0.33	169.4743	119.8101	98.58128

(c) Read the values on the two instruments;
(d) Disassembly the heat exchanger from the compressor input and output;

5.5. Organic rankine fluid campaign results

Following the procedure described above, the temperature range and pressure losses, for each of the exchangers, have been measured and all data processed. Tables 11 and 12 show all results.

6. Results analysis and comparison

Once the tests were completed and all data collected, the next step was to analyze these data for choosing the optimal exchanger configuration. Experimental tests have proved that the two most influencing factors are the fluid density and viscosity. Table 13 shows the different refrigerants density and dynamic viscosity. From the analysis of Re values, the viscosity value (linked to the passage from laminar to turbulent) determines quite clearly the optimal exchanger configuration. In fact, in turbulent mode the optimum configuration is the constant-speed configuration, while in laminar regime the constructal one is slightly better (the values are very close), if the viscosity of the fluid is high. In the other case, constant-speed configuration turns out to be the optimal one, but also the constructal solution is very close. For this reason, both solutions are reported, indicating with a "+" the configuration with the highest values. Finally, more increases the fluid flow-rate more increases, exponentially, the thermal efficiency.

These considerations allow compiling Table 14, indicating the optimal match between fluid and branched configuration.

In addition, to better understand and evaluate the process, have been calculated the different Reynolds, Prandtl numbers for common refrigerants fluid and for R134 organic fluid. All results are reported in Tables 15 and 16, respectively

Successively, the Nusselt number is computed using the following formulae [15] (Tables 17 and 18, respectively):

Laminar

$$\overline{Nu}_D = 3.66 + \frac{0.0668\ (D/L)\ Re_D\ Pr}{1 + 0.04[(D/L)\ Re_D\ Pr]^{2/3}}$$

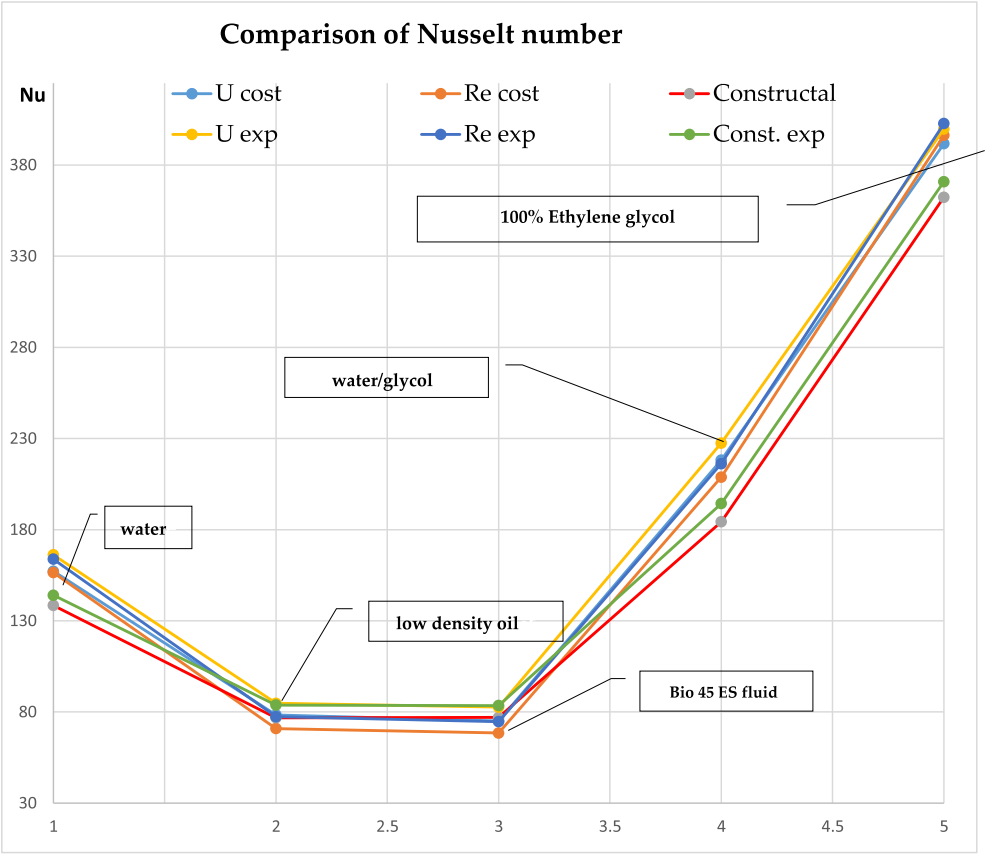

Fig. 8. Comparison of Nusselt number (calculated and experimental).

Turbulent

$$(L/D) < 60 \;\rightarrow\; \overline{Nu}_D \;\approx\; \overline{Nu}_{D,fd} \approx \left[\frac{1+C}{(L/D)^{2/3}}\right] \quad \text{with } C \approx 1$$

The fluid viscosity is strictly connected to the laminar or turbulent flow, and optimum heat exchange is achieved in this efflux regime. The Prandtl number calculation shows that (see Fig. 8), due to the minimal change in the fluid properties, the results do not change. This consideration can apply to every fluid for each exchanger configurations and mass-flow rates. Therefore, the variation of the momentum of the fluid is greater than the thermal flux, which occurs by diffusivity. The heat is exchanged much slower than the momentum. The thermal contour is contained within the boundary layer. Finally, by calculating the Nusselt number, due to its minimal variability, it shows how the results have the same tendency as the Reynolds results.

7. Conclusions and future developments

The aim of this paper was the determination of the best configuration for a branched heat exchanger. Different fluids, including organic one, have been considered. During the experimental campaign, 3 exchangers (configuration A, B and C) with 4 (four) operating fluids and 1 (one) organic fluid have been tested, by varying the flow-rate. Thanks to these tests, a strong correlation has been found between fluid viscosity and exchanger configuration. Considering common coolant fluids, in laminar regime and low viscosity, the constant-speed configuration results the optimal one (the constructal is very close), whilst at high viscosity, the constructal solution turns out to be the optimal one (in this case the constant-speed solution is close to it). In turbulent flux, the constant-speed solution is the optimal solution. Regarding the test carried out with the organic fluid, the optimal/compromise solution is almost the configuration A (constant-speed configuration), ensuring optimal cooling performance, independent of the Re numbers. The problem with such a fluid concerns the constructive and safety issues. To assemble the system, the circuit must be under vacuum. In addition, the fluid refilling system must be carefully studied. A further feature of these fluids concerns flammability and pollution. For this reason, the realization of a sealed circuit and the respect of all safety standards is mandatory. Finally, future developments are connected to the solution of these problems, and their possible application, that could be in the field of microelectronics, i.e. for the CPUs cooling.

Declaration of Competing Interest

The authors declared that there is no conflict of interest.

References

[1] A. Heitor Reis, Constructal theory: from engineering to physics, and how flow systems develop shape and structure, Appl. Mech. Rev. 59 (5) (2006) 269–282.
[2] A. Bejan, Shape and Structure, From Engineering to Nature, Cambridge, Cambridge University Press, 2000. ISBN: 9780521793889.
[3] A. Bejan, Advanced Engineering Thermodynamics, second ed., Wiley, New York, 1997. ISBN-13: 978-0471677635; ISBN-10: 0471677639.
[4] W. Wechsatol, S. Lorente, A. Bejan, Tree-shaped flow structure: are both thermal-resistance and flow-resistance minimization necessary? Int. J. Exergy 1(1) (2004). DOI: http://dx.doi.org/10.1504/IJEX.2004.004731.
[5] R. Capata, A. Beyene, Experimental evaluation of three different configurations of constructal disc-shaped heat exchangers, Int. J. Heat Mass Transf. 115 (2017) 92–101, https://doi.org/10.1016/j.ijheatmasstransfer.2017.06.096.
[6] ISO International Organization for Standardization, Guide to the Expression of Uncertainty in Measurement, second ed., Geneva 1995. ISBN 92-67-10188-9.
[7] R. Kacker, A. Jones, On use of Bayesian statistics to make the Guide to the Expression of Uncertainty in Measurement consistent, National Institute of Standards and Technology, Gaithersburg, MD 20899-8910, USA.
[8] http://chapon.arnaud.free.fr/documents/resources/stat/GUM.pdf (visited January 2016).
[9] N. Barry, Taylor and Chris E. Kuyatt, NIST Technical Note 1297, 1994 Edition, Guidelines for Evaluating and Expressing the Uncertainty of NIST Measurement Results.
[10] M. Robbe, E. Sciubba, A CFD-aided design procedure for compact heat exchangers, in: ECOS 2005 – Proceedings of the 18th International Conference on Efficiency, Cost, Optimization, Simulation, and Environmental Impact of Energy Systems (ECOS 2005), Tapir Academic Press, pages 1415–1425, ISBN8251920418.
[11] M. Robbe, E. Sciubba, An industrial application of constructal theory: a constructal CPU liquid cooling unit, in: Proceedings of ASME IMECE2008 International Mechanical Engineering Congress and Exposition, Boston, MA (US), 2008, Vol. 10, pp. 1541–1552.
[12] A. Cancellario, L. Nana, E. Sciubba, EL-COOL: an innovative ultra-micro cooling system for CPU racks part I-II, in: Proceedings of ECOS 2018, Guimaraes, Portugal, June 17–21 2018.
[13] A. Cancellario, A possible ultra-micro cooling system for high performance CPU based on Nano-Heat Exchangers, in: Proceedings of ECOS 2017, San Diego (USA), July 02–06 2017.
[14] D. Ziviani, A. Beyene, Venturini, Design, analysis and optimization of a micro-ORC system based on Organic Rankine Cycle for ultralow grade thermal energy recovery, JERT-12-1288, 136(1), pp. 1–11.
[15] K. Thulukkanam, Heat Exchanger Design Handbook, CRC Press. Taylor & Francis Inc. April 2017, ISBN 9781138074668.